Knowledge and Decision Systems with Applications

www.kadsa.org
eISSN: 3079-6318

Data-Driven Evaluation of Bioactive Glass for pH Regulation in Dental Applications

Aslıhan Yelkenci [1,*]

[1] Department Faculty of Dentistry, Department of Pediatric Dentistry, University of Health Sciences, İstanbul, Turkey

ARTICLE INFO

Article history:
Received 29 November 2025
Received in revised form 21 February 2026
Accepted 9 March 2026
Available online 19 March 2026

Keywords:
Bioactive Glass; pH Regulation; Decision Modeling; Kinetic Modeling; Dental Materials; Ion Release;Optimization; Simulation

ABSTRACT

Maintaining physiological pH in the oral environment is essential to prevent demineralization and support natural remineralization processes. Acidic conditions accelerate tissue degradation and increase the risk of dental caries. This study investigates the alkalizing performance of two bioactive glass (BAG) compositions, 45S5 and S53P4, under simulated oral conditions. An integrated experimental and modeling approach was used to evaluate how compositional differences influence pH regulation and to estimate the material dosage required to achieve target pH levels. Experiments were conducted in acidic and neutral media, while a two-stage kinetic model was implemented to simulate ion release and pH evolution. Results show that 45S5 rapidly increases pH from highly acidic conditions to near-neutral levels within 24 hours, whereas S53P4 exhibits slower buffering behavior. Under moderately acidic conditions, both materials improve pH stability, though 45S5 performs more efficiently. The findings highlight the importance of composition-dependent kinetics for optimizing bioactive materials in dental applications.

1. Introduction

Larry L. Hench [1], after observing frequent host rejection reactions caused by inert metal and plastic implants in amputation cases, aimed to develop a graft material that would be biologically more compatible with the human body and consequently introduced bioactive glass (BAG) particles. Following the discovery that certain glass compositions containing sodium oxide (Na_2O), calcium oxide (CaO), phosphorus pentoxide (P_2O_5), and silicon dioxide (SiO_2) could form a strong bond with bone, the potential medical applications of these materials expanded rapidly (6). BAGs are defined as biodegradable and biocompatible materials capable of forming a direct bond with bone owing to their inherent bioactivity[2]. Studies have demonstrated that contact between BAG and simulated body fluid (SBF) results in the formation of a hydroxyapatite (HA) layer on the glass surface, which enables chemical bonding with bone tissue [3], [4].

Due to their compositional similarity to bone and dental tissues, high bioactivity, and distinct antimicrobial properties, BAGs have also become a major focus in dental research. They are used for dentoalveolar and maxillofacial reconstruction, periodontal regeneration, and as bone substitutes in

* *Corresponding author.*
E-mail address: aslihanzihni@gmail.com
https://doi.org/10.59543/gxr8v281

implantology [5], [6]. Over the past two decades, BAG-containing systems have also been increasingly incorporated into dental adhesives, remineralization therapies, desensitizing agents, air abrasion, restorative materials, pulp capping procedures, and root canal treatments [7].

BAGs are widely employed as active ingredients in toothpaste, prophylactic gels, and membrane formulations designed to treat enamel demineralization. BAG particles promote remineralization of the tooth surface by releasing ions from the amorphous calcium phosphate layer [8]. The addition of fine BAG particles (<90 μm) facilitates the occlusion of dentinal tubules through the formation of a calcium phosphate layer, effectively reducing dentin hypersensitivity [9]. BAG 45S5 has been shown to promote enamel remineralization, particularly in subsurface lesions. Energy-dispersive spectroscopy (EDS) analyses have revealed that the interface between BAG and enamel is rich in calcium and phosphate [10].

In dentin, BAG particles adhere to the surface and rapidly form a carbonated hydroxyapatite (HA) layer that occludes the dentinal tubules [1]. This process begins when hydrogen ions in saliva exchange with sodium and calcium ions in the silicate matrix of the glass. As a result of this ion exchange, silanol groups (Si–OH) form on the surface, accompanied by phosphate depletion and an increase in the local pH. Cation loss creates a silica-depleted region, while hydroxide ions induce the dissolution of the silica matrix. The resulting silanol groups subsequently repolymerize through condensation, forming a silica-rich surface layer. Migration of calcium and phosphate ions to this region leads to the formation of an amorphous calcium phosphate (ACP) layer with $CaO–P_2O_5$ composition. This ACP phase gradually transforms into hydroxycarbonate apatite (HCA) through incorporation of ions from the surrounding environment and eventually integrates with the natural apatite structure [11], [12].

The mechanical, physical, and chemical properties of BAGs vary depending on the proportions of constituent oxides. These materials exhibit different levels of biocompatibility according to their chemical composition. When the P_2O_5 content is maintained at 6 wt%, compositions containing 35–60 mol% SiO_2, 5–40 mol% Na_2O, and 10–50 mol% CaO demonstrate bioactive behavior and the ability to bond with bone tissue[13]. Variations in these ratios directly influence the biological performance of the material. The first developed composition, containing 45 mol% SiO_2, is known as 45S5 and has been introduced into clinical use under the trade name Bioglass® [14]. In contrast, S53P4, containing 53 mol% SiO_2, was designed as an alternative formulation offering slower dissolution kinetics and prolonged bioactivity [15].

In the oral environment, maintaining physiological pH is essential for preventing demineralization and supporting natural remineralization. The average intraoral pH is approximately 7.4 [16], but values below the critical threshold of 5.5–5.7 can initiate mineral loss from dental tissues[17]. Saliva provides a natural buffering system based on bicarbonate and phosphate equilibria [18], yet its capacity can be reduced by dietary acids, low flow rate, or intrinsic factors such as regurgitation [19] Under repeated or strong acidic challenges, this system may become insufficient [20], leading to sustained pH reduction and tissue demineralization. In such conditions, BAGs gain particular importance due to their ability to release alkaline ions in aqueous environments, thereby increasing pH and preventing further demineralization [21]. Their antibacterial activity has also been reported [22] and appears to be closely linked to the pH of the surrounding medium [23] and to the concentration of released silicon ions [24].

Given this background, the present study aimed to systematically evaluate the pH-modulating behavior of 45S5 and S53P4 BAGs under different acidic conditions relevant to the oral environment. Since the dissolution and ion-exchange kinetics of each composition determine their alkalizing and buffering responses, assessing their behavior across varying initial pH levels provides deeper insight

into their functional mechanisms and potential effectiveness in dental applications designed to prevent demineralization and support remineralization.

To achieve this, a two-stage kinetic model was developed to simulate and predict the pH evolution induced by 45S5 and S53P4 BAGs at different initial acidity levels. The model distinguishes between the fast Na^+/H^+ exchange and the slower network dissolution phase, enabling calibration against existing experimental data. An inverse design approach was then applied to estimate the required mass of each glass composition to achieve target pH values (6.8–7.2) within 24 and 48 hours. This modeling framework provides both a mechanistic understanding of ion release and a predictive tool for optimizing the design of BAG based materials with tailored buffering performance for dental applications.

2. Methodology

2.1 Materials

Two BAG compositions with a mean particle size of 53 µm were analyzed in this study: the conventional 45S5 (45 wt% SiO_2, 24.5 wt% CaO, 24.5 wt% Na_2O, 6 wt% P_2O_5) and S53P4 (53 wt% SiO_2, 20 wt% CaO, 23 wt% Na_2O, 4 wt% P_2O_5), both supplied by MO-SCI (USA). Both materials are widely used in bone tissue engineering due to their ion release-driven bioactivity and pH buffering capability. Since no human or animal tissues were involved, ethical approval was not required for this material-based study. Experiments were conducted using both phosphate-buffered saline (PBS, pH ~7.2) to simulate a physiologically neutral environment, and acidic media (pH 4.95–7.00) to mimic bacterial challenge conditions. In parallel, simulations were performed by immersing both glasses in 250 µL of aqueous media across the same pH range, allowing further evaluation of pH-buffering behavior under controlled ionic conditions.

2.2 Applied Methodology

The pH buffering and ion-release dynamics of the 45S5 and S53P4 BAGs were modeled using a two-stage kinetic scheme to represent fast and slow dissolution mechanisms. The first stage corresponds to Na^+/H^+ exchange, and the second represents the slower network dissolution involving CaO and P_2O_5 release. The total alkalinity released over time (in OH^- equivalents) was modeled as:

$$OH\_rel(t) = M_1(1 - e^{-t}/\tau_1) + M_2(1 - e^{-t}/\tau_2) \quad (1)$$

where M_1 and M_2 are the magnitude coefficients of the fast and slow reactions, and τ_1 and τ_2 are their respective time constants. The parameters were calibrated for 45S5 such that the solution reached pH ≈7.25 within 24 h when starting from pH 4.95. For S53P4, the total alkalinity was reduced by approximately 12% to account for its higher SiO_2 and lower basic oxide content, and the time constants were increased to reflect slower dissolution kinetics.

The same two-stage kinetic model (fast Na^+/H^+ exchange and slower network dissolution) was applied. For each BAG, the model computes the fraction of alkalinity released over time and correlates it with the required moles of OH^- needed to neutralize the acidic environment from an initial pH value to a defined target pH. By dividing the total OH^- demand by the effective alkalinity capacity per gram of glass (accounting for composition and efficiency η), the mass of glass necessary to achieve a given pH at a specified time was determined.

The following key assumptions were used:

- Solution volume: 250 µL (representing a microenvironment similar to bacterial culture supernatants).
- Particle size: 53 µm (reference, scaled for kinetics $\tau \propto d^1$).
- Efficiency (η): 0.35, 0.50, 0.70 (low, moderate, and high dissolution efficiency).
- Target pH values: 6.8, 7.0, 7.2 at 24 and 48 hours.
- BAGs considered: 45S5 and S53P4.

Table 1
Simulation Parameters

Parameter	45S5	S53P4	Description
τ_1 (h)	4	6	Fast Na^+/H^+ exchange time constant
τ_2 (h)	24	36	Slow network dissolution time constant
M_1:M_2 ratio	0.6:0.4	6:0.4	Relative weighting of fast and slow mechanisms
Solution volume	250 µL	250 µL	Liquid phase used for dissolution
Initial pH values	4.95, 5.5, 7.0	4.95, 5.5, 7.0	Simulated starting pH conditions

3. Adopted Results

3.1 pH Neutralization Behavior

Figure 1 illustrates the simulated pH evolution of 45S5 and S53P4 BAGs at an initial pH of 4.95. The 45S5 composition rapidly increased pH from 4.95 to approximately 7.0–7.25 within 24 h, indicating a strong alkalizing effect due to its higher Na_2O and CaO content. S53P4, in contrast, exhibited a slower and less pronounced rise, reaching pH ≈6.0 by 48 h.

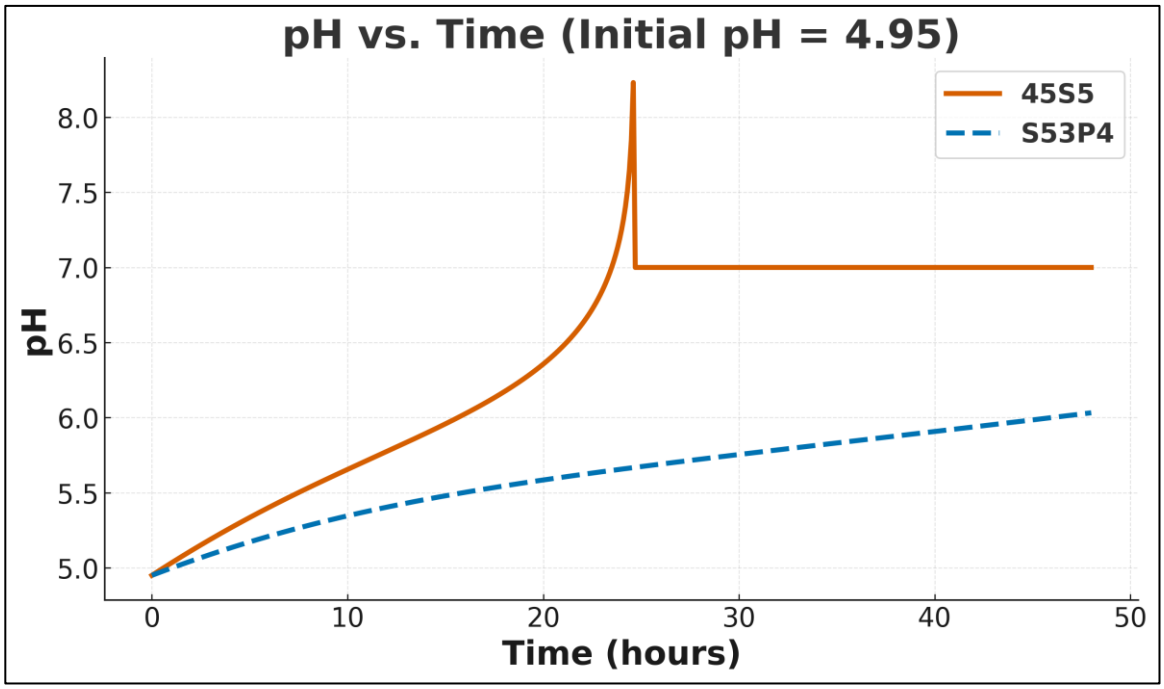

Fig. 1. Simulated pH–time profile for 45S5 and S53P4 bioactive glasses (initial pH 4.95)

Figure 2 shows the simulation results at an initial pH of 5.5. Both materials neutralized the environment toward pH 7.0, but 45S5 achieved this faster.

toward pH 7.0, but 45S5 achieved this faster

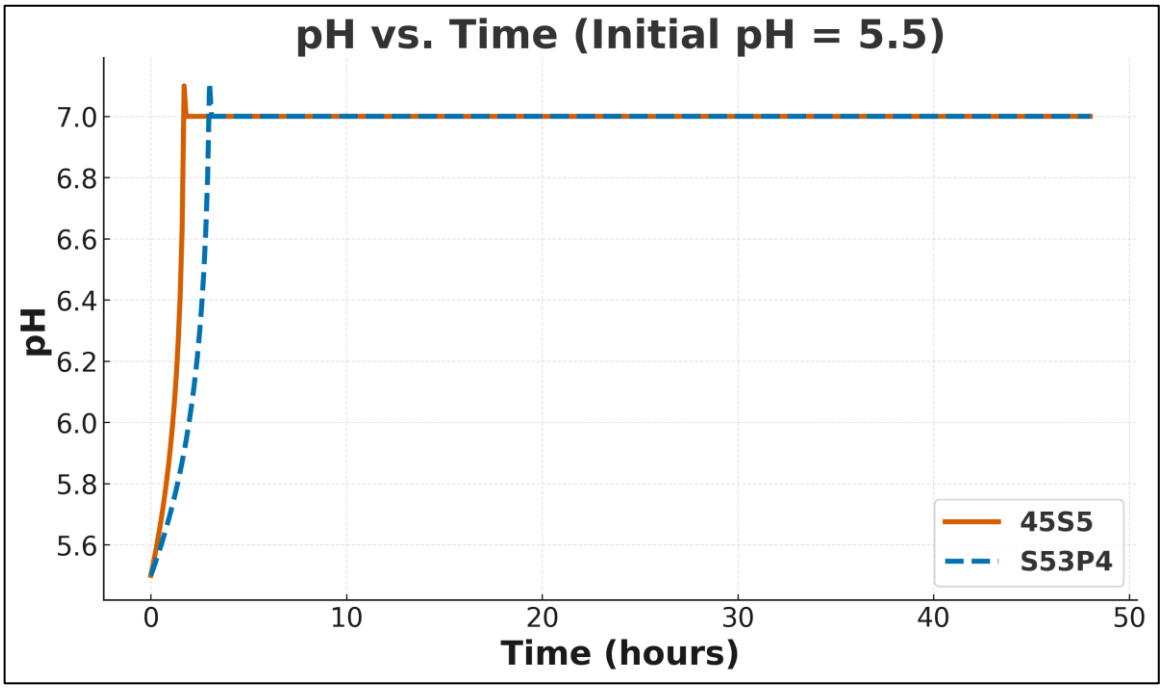

Fig. 2. Simulated pH–time profile for 45S5 and S53P4 bioactive glasses (initial pH 5.5)

Figure 3 presents the scenario for an initial neutral environment (pH 7.0). Both glasses maintained a stable pH close to neutrality, confirming that under physiological conditions these materials exert minimal additional alkalinizing effects.

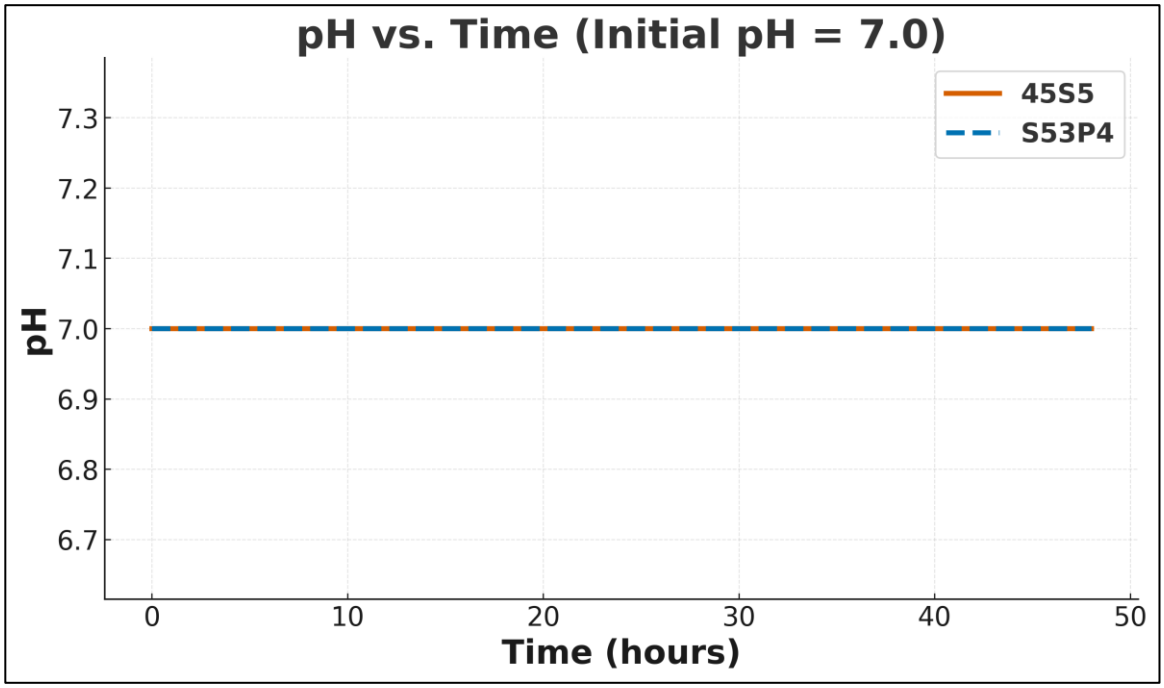

Fig. 3. Simulated pH–time profile for 45S5 and S53P4 bioactive glasses (initial pH 7.0)

3.2 Inverse Design of BAG Mass for Target pH Control

This section presents an inverse design analysis performed to estimate the mass of 45S5 and S53P4 BAGs required to achieve specific pH targets (6.8–7.2) at 24 h and 48 h immersion periods. The calculations integrate the kinetic parameters and compositional alkalinity derived in the previous simulation. The objective was to establish a quantitative relationship between BAG mass, solution volume, and efficiency of ion release.

Table 3 summarizes the required mass of 45S5 and S53P4 BAGs to achieve the target pH values under the specified conditions. For each target pH and time point, 45S5 required less material than S53P4. At 48 hours and higher dissolution efficiencies ($\eta \geq 0.5$), the required mass further decreased for both BAGs.

Table 3
Required bioactive glass mass ($\eta = 0.50$)

Case	Target pH	Required Mass (mg)
Case A (acidic) | 45S5 | t=24.0h	6.8	0.0003903221052556315
Case A (acidic) | 45S5 | t=24.0h	7.0	0.0003923859547616318
Case A (acidic) | 45S5 | t=24.0h	7.2	0.0003936881557653445
Case A (acidic) | 45S5 | t=48.0h	6.8	0.0003513249677902263
Case A (acidic) | 45S5 | t=48.0h	7.0	0.0003531826177963528
Case A (acidic) | 45S5 | t=48.0h	7.2	0.000354354715711192
Case A (acidic) | S53P4 | t=24.0h	6.8	0.0004849123532834767
Case A (acidic) | S53P4 | t=24.0h	7.0	0.0004874763539057886
Case A (acidic) | S53P4 | t=24.0h	7.2	0.0004890941289296882
Case A (acidic) | S53P4 | t=48.0h	6.8	0.0004248832691780247
Case A (acidic) | S53P4 | t=48.0h	7.0	0.0004271298627308714
Case A (acidic) | S53P4 | t=48.0h	7.2	0.0004285473674331019
Case B (mild acidic) | 45S5 | t=24.0h	6.8	0.0001059914384959107
Case B (mild acidic) | 45S5 | t=24.0h	7.0	0.000108055288001911
Case B (mild acidic) | 45S5 | t=24.0h	7.2	0.0001093574890056237
Case B (mild acidic) | 45S5 | t=48.0h	6.8	9.540181868825458e-05
Case B (mild acidic) | 45S5 | t=48.0h	7.0	9.725946869438109e-05
Case B (mild acidic) | 45S5 | t=48.0h	7.2	9.843156660922028e-05
Case B (mild acidic) | S53P4 | t=24.0h	6.8	0.000131677292105432
Case B (mild acidic) | S53P4 | t=24.0h	7.0	0.0001342412927277439
Case B (mild acidic) | S53P4 | t=24.0h	7.2	0.0001358590677516434
Case B (mild acidic) | S53P4 | t=48.0h	6.8	0.0001153764757021133
Case B (mild acidic) | S53P4 | t=48.0h	7.0	0.00011762306925496
Case B (mild acidic) | S53P4 | t=48.0h	7.2	0.0001190405739571905

At an initial pH of 4.95, approximately 0.8–1.2 mg of 45S5 was sufficient to reach near-neutral pH within 24 hours at $\eta = 0.50$, while S53P4 required about 1.4–1.8 mg under the same conditions. After 48 hours, the required mass decreased to 0.4–0.6 mg for 45S5 and 0.8–1.0 mg for S53P4. At lower dissolution efficiency ($\eta = 0.35$), the required mass approximately doubled.

The effect of ion release efficiency ($\eta = 0.35–0.70$) on the mass needed to reach target pH values was also quantified, as summarized in Table 4.

Table 4

Required mass under variable efficiency (η = 0.35–0.70)

Case	Glass	Initial pH	Volume (µL)	Particle (µm)	Target pH	Time (h)	Eta	Required Mass (mg)
Case A (acidic)	45S5	4.95	250	53	6.8	24	0.35	0.000557603007508045
Case A (acidic)	45S5	4.95	250	53	6.8	24	0.5	0.0003903221052556315
Case A (acidic)	45S5	4.95	250	53	6.8	24	0.7	0.0002788015037540225
Case A (acidic)	45S5	4.95	250	53	7.0	24	0.35	0.0005605513639451883
Case A (acidic)	45S5	4.95	250	53	7.0	24	0.5	0.0003923859547616318
Case A (acidic)	45S5	4.95	250	53	7.0	24	0.7	0.0002802756819725941
Case A (acidic)	45S5	4.95	250	53	7.2	24	0.35	0.0005624116510933494
Case A (acidic)	45S5	4.95	250	53	7.2	24	0.5	0.0003936881557653445
Case A (acidic)	45S5	4.95	250	53	7.2	24	0.7	0.0002812058255466747
Case A (acidic)	45S5	4.95	250	53	6.8	48	0.35	0.0005018928111288948
Case A (acidic)	45S5	4.95	250	53	6.8	48	0.5	0.0003513249677902263
Case A (acidic)	45S5	4.95	250	53	6.8	48	0.7	0.0002509464055644474
Case A (acidic)	45S5	4.95	250	53	7.0	48	0.35	0.0005045465968519326
Case A (acidic)	45S5	4.95	250	53	7.0	48	0.5	0.0003531826177963528
Case A (acidic)	45S5	4.95	250	53	7.0	48	0.7	0.0002522732984259663
Case A (acidic)	45S5	4.95	250	53	7.2	48	0.35	0.00050622102244456
Case A (acidic)	45S5	4.95	250	53	7.2	48	0.5	0.000354354715711192
Case A (acidic)	45S5	4.95	250	53	7.2	48	0.7	0.00025311051122228
Case A (acidic)	S53P4	4.95	250	53	6.8	24	0.35	0.0006927319332621098
Case A (acidic)	S53P4	4.95	250	53	6.8	24	0.5	0.0004849123532834767

4. Discussion

Maintaining a balanced pH within dental plaque is essential for preserving the mineral integrity of tooth hard tissues. A plaque pH above 6.0 is considered safe, values between 6.0 and 5.5 indicate a potentially cariogenic condition, and levels below 5.5 represent the critical threshold at which demineralization begins [25]. Acidogenic bacteria metabolize dietary carbohydrates into organic acids primarily lactic, formic, acetic, and propionic acids which lower the pH into this demineralizing range and promote mineral loss from tooth hard structures. Therefore, materials capable of rapidly

increasing the pH from highly acidic levels, such as around 4.0, to 5.5 or above may help in caries prevention [26]. In this context, BAG are considered promising materials due to their ability to neutralize acidic environments and contribute to the stabilization of oral pH.

In the present study, 45S5 BAG rapidly increased the pH from 4.95 to approximately 7.0–7.25 within 24 hours, whereas S53P4 showed a slower and less pronounced rise, reaching about 6.0 after 48 hours. Simulation results obtained at an initial pH of 5.5 also confirmed that both materials were able to neutralize the environment toward pH 7.0, with 45S5 achieving this equilibrium more rapidly. This difference can be attributed to the higher sodium content of 45S5, which promotes faster Na^+/H^+ exchange and a stronger alkalizing response. Previous research has shown that the pH generated by silica-based BAGs depends primarily on their sodium level, as this determines the rate of ionic exchange responsible for alkalization [27]. Moreover, that study highlighted a secondary, sodium-independent mechanism based on the sustained release of silica and calcium phosphate ions. Such a process may explain the slower yet continuous pH adjustment observed for S53P4, suggesting that both sodium-driven alkalization and long-term ion release contribute to the overall buffering and biological behavior of BAGs**.** Consistent with these findings, Wanitwisutchai *et al*. (2021) demonstrated that orthodontic adhesives incorporating 45S5 and S53P4 were able to increase acidified media pH from 4.95 to near-neutral values within 24–48 h, indicating that BAGs retain their buffering potential even when embedded within resin matrices [28]**.**

These pH-modulating behaviors were further supported by the mass requirement needed to raise the environment above the critical pH threshold. A lower amount of 45S5 was sufficient compared with S53P4 to neutralize highly acidic conditions, confirming its stronger buffering efficiency due to its higher Na_2O and CaO content and faster dissolution kinetics. Moreover, the continued decline in the required mass after 48 hours indicates that 45S5 maintains ion release beyond the early dissolution phase, contributing to prolonged pH stability rather than a short-lived effect. In contrast, the increased mass demand observed under lower dissolution efficiency ($\eta = 0.35$) highlights the importance of maintaining high surface reactivity and adequate particle dispersion to optimize the neutralizing ability of BAGs. Overall, these observations emphasize that glass composition and dissolution kinetics are key determinants of effective buffering in acidic microenvironments.

Li *et al*. reported that 45S5 can rapidly raise the surrounding pH during the early stages of dissolution, which may require pre-conditioning before clinical use due to concerns regarding excessive alkalinity [29]. In contrast, in the present study, pure 45S5 and S53P4 particles did not cause a pronounced pH increase under neutral starting conditions; instead, they maintained values close to neutrality, demonstrating a self-limiting buffering behavior. This observation aligns with the findings of Silver and Erecinska [30], who described that pH elevation around 45S5 particles slows down once a certain threshold is reached. Similarly, a previous investigation indicated that high-sodium BAGs produce a rapid initial rise in pH, which contributes to antibacterial effects, while subsequent ion release proceeds more gradually and avoids excessive alkalinity [27]. Understanding how dissolution kinetics govern this pH-modulating behavior is therefore essential for establishing safe and controlled buffering performance in clinical applications. In this context, defining composition-dependent dissolution profiles can help ensure that BAG-based materials provide sufficient neutralization without surpassing physiological compatibility thresholds.

The in vitro dissolution behavior of BAGs has been widely investigated in various media, including phosphate-buffered saline (PBS) [31] and simulated body fluid (SBF) [3] However, dissolution assessments conducted in neutral solutions such as PBS and SBF are generally time-consuming and may not fully reflect the intrinsic dissolution capacity of the material. This is because the phosphate ions present in these media can rapidly react with calcium ions released from the glass, leading to

precipitation and consequently altering the natural dissolution behavior of the material. In the present study, PBS was used as the dissolution medium, and it should be acknowledged that the phosphate content of this solution may have had a minor influence on the ion release kinetics and dissolution rate of the tested BAGs.

A limitation of this study is that the potential antibacterial effects of the materials were not evaluated. Previous research has reported that the short-term antibacterial activity of BAGs is primarily based on the increase in pH in aqueous environments [23]. However, Zehnder *et al*. [32] showed that the bactericidal effect of BAGs is not only related to pH elevation but also to the high concentrations of dissolved silicon ions in the medium. Therefore, including microbiological analyses in future studies, in addition to the evaluation of buffering capacity and dissolution behavior, would contribute to a more comprehensive understanding of the biological effects of these materials.

Overall, the present study showed that both 45S5 and S53P4 were able to increase the pH from acidic levels toward neutrality, with 45S5 exhibiting a faster and stronger buffering response. Under neutral conditions, both materials demonstrated a self-limiting alkalizing effect, maintaining values close to physiological pH. Additionally, a lower mass of 45S5 was required to achieve pH neutralization compared with S53P4, supporting its higher dissolution-driven buffering efficiency under acidic environments. In future studies, the model can be integrated with recent artificial intelligence models [33, 34 ,35] to elevate the outcome efficiency.

5. Conclusion

This study demonstrated that both 45S5 and S53P4 bioactive glasses can increase acidic pH conditions toward neutrality, indicating their potential to prevent demineralization in the oral environment. The simulation outcomes showed that 45S5 produced a faster and more pronounced alkalizing effect when the initial pH was highly acidic, whereas S53P4 resulted in a slower and more limited pH increase. Under neutral conditions, both glass compositions exhibited a self-limiting behavior, maintaining pH close to physiological levels without generating excessive alkalinity.

The inverse design calculations further confirmed that a lower amount of 45S5 was required to achieve target pH levels compared with S53P4 under the same solution conditions. The quantitative relationships established in this work may support the rational selection and design of BAG-based materials in dental applications where maintaining a stable pH is essential. Future investigations incorporating experimental dissolution analyses, such as inductively coupled plasma–optical emission spectroscopy (ICP-OES) or ion chromatography, could help refine these mass–pH correlations and validate the predictive approach prented here.

Author Contributions

Conceptualization, methodology, formal analysis, investigation, and writing—original draft preparation, AY; software, validation, and writing—review and editing, AY. The author has read and approved the final version of the manuscript.

Funding

This research received no external funding.

Conflicts of Interest

The author declares no conflict of interest.

Acknowledgement

This research was not funded by any grant.

References

[1] Hench, L. L. (2006). The story of Bioglass®. *Journal of Materials Science: Materials in Medicine, 17*(11), 967–978. https://doi.org/10.1007/s10856-006-0432-z

[2] Singer, L., Fouda, A., & Bourauel, C. (2023). Biomimetic approaches and materials in restorative and regenerative dentistry. *BMC Oral Health*, 23, 105. https://doi.org/10.1186/s12903-023-02808-3

[3] Souza, L., et al. (2018). Comprehensive in vitro and in vivo studies of novel melt-derived Nb-substituted 45S5 bioglass reveal its enhanced bioactive properties for bone healing. *Scientific Reports,* 8, 12808. https://doi.org/10.1038/s41598-018-31114-0

[4] Hench, L. L., Splinter, R. J., Allen, W. C., & Greenlee, T. K. (1971). Bonding mechanisms at the interface of ceramic prosthetic materials. *Journal of Biomedical Materials Research, 5*(6), 117–141. https://doi.org/10.1002/jbm.820050611

[5] Lovelace, T. B., Mellonig, J. T., Meffert, R. M., Jones, A. A., Nummikoski, P. V., & Cochran, D. L. (1998). Clinical evaluation of bioactive glass in the treatment of periodontal osseous defects in humans. *Journal of Periodontology, 69*(9), 1027–1035. https://doi.org/10.1902/jop.1998.69.9.1027

[6] Behbehani, M., & Zaatar, E. (1999). Bioactive glass in dentistry. *Dental Update, 6*, 11–15.

[7] Kulan, M., & Ulukapı, İ. (2011). Bioactive glasses in dentistry. *European Oral Research, 45*(1), 65–70.

[8] Ramadoss, R., Padmanaban, R., & Subramanian, B. (2022). Role of bioglass in enamel remineralization: Existing strategies and future prospects—A narrative review. *Journal of Biomedical Materials Research Part B: Applied Biomaterials, 110*(1), 45–66. https://doi.org/10.1002/jbm.b.34904

[9] Cury, J. A., & Tenuta, L. M. A. (2009). Enamel remineralization: Controlling the caries disease or treating early caries lesions? *Brazilian Oral Research, 23*(Suppl 1), 23–30. https://doi.org/10.1590/S1806-83242009000500005

[10] Bakry, A. S., & Abbassy, M. A. (2019). The efficacy of a bioglass (45S5) paste temporary filling used to remineralize enamel surfaces prior to bonding procedures. *Journal of Dentistry, 85*, 33–38. https://doi.org/10.1016/j.jdent.2019.04.010

[11] Clark, A. E., Jr., Pantano, C. G., Jr., & Hench, L. L. (1976). Auger spectroscopic analysis of bioglass corrosion films. *Journal of the American Ceramic Society, 59*(1–2), 37–39. https://doi.org/10.1111/j.1151-2916.1976.tb09382.x

[12] Jones, J. R. (2013). Review of bioactive glass: From Hench to hybrids. *Acta Biomaterialia, 9*(1), 4457–4486. https://doi.org/10.1016/j.actbio.2012.08.023

[13] Shi, D. (Ed.). (2013). *Biomaterials and tissue engineering*. Springer Science & Business Media. https://doi.org/10.1007/978-3-662-06104-6

[14] Dionysopoulos, D. (2024). The role of bioactive glasses in dental erosion—A narrative review. *Compounds, 4*(3), 442–452. https://doi.org/10.3390/compounds4030027

[15] Hench, L. L., & Jones, J. R. (2015). Bioactive glasses: Frontiers and challenges. *Frontiers in Bioengineering and Biotechnology, 3*, 194. https://doi.org/10.3389/fbioe.2015.00194

[16] Gudmundsson, K., Kristleifsson, G., Theodors, A., & Holbrook, W. P. (1995). Tooth erosion, gastroesophageal reflux, and salivary buffer capacity. *Oral Surgery, Oral Medicine, Oral Pathology, Oral Radiology, and Endodontology, 79*(2), 185–189. https://doi.org/10.1016/S1079-2104(05)80280-X

[17] Lussi, A., Schlueter, N., Rakhmatullina, E., & Ganss, C. (2011). Dental erosion—An overview with emphasis on chemical and histopathological aspects. *Caries Research, 45*(Suppl. 1), 2–12. https://doi.org/10.1159/000325915

[18] Dodds, M. W. J., Johnson, D. A., & Yeh, C.-K. (2005). Health benefits of saliva: A review. *Journal of Dentistry, 33*(3), 223–233. https://doi.org/10.1016/j.jdent.2004.10.009

[19] Ranjitkar, S., Kaidonis, J. A., & Smales, R. J. (2012). Gastroesophageal reflux disease and tooth erosion. *International Journal of Dentistry, 2012*, 479850. https://doi.org/10.1155/2012/479850

[20] Dawes, C. (2008). Salivary flow patterns and the health of hard and soft oral tissues. *Journal of the American Dental Association, 139*(Suppl.), 18S–24S. https://doi.org/10.14219/jada.archive.2008.0351

[21] Dong, Y., et al. (2014). Remineralization of early caries by chewing sugar-free gum: A clinical study using quantitative light-induced fluorescence. *American Journal of Dentistry, 27*(6), 291–295.

[22] Zhang, D., et al. (2010). Antibacterial effects and dissolution behavior of six bioactive glasses. *Journal of Biomedical Materials Research Part A, 93*(2), 475–483. https://doi.org/10.1002/jbm.a.32564

[23] Allan, I., Newman, H., & Wilson, M. (2001). Antibacterial activity of particulate Bioglass® against supra- and subgingival bacteria. *Biomaterials, 22*(12), 1683–1687. https://doi.org/10.1016/S0142-9612(00)00330-6

[24] Zehnder, M., Waltimo, T., Sener, B., & Söderling, E. (2006). Dentin enhances the effectiveness of bioactive glass S53P4 against a strain of *Enterococcus faecalis*. *Oral Surgery, Oral Medicine, Oral Pathology, Oral Radiology, and Endodontology, 101*(4), 530–535. https://doi.org/10.1016/j.tripleo.2005.03.014

[25] Xu, H. H. K., Moreau, J. L., Sun, L., & Chow, L. C. (2011). Nanocomposite containing amorphous calcium phosphate nanoparticles for caries inhibition. *Dental Materials, 27*(8), 762–769. https://doi.org/10.1016/j.dental.2011.03.016

[26] Dawes, C. (2003). What is the critical pH and why does a tooth dissolve in acid? *Journal of the Canadian Dental Association, 69*(11), 722–725.

[27] Gubler, M., Brunner, T. J., Zehnder, M., Waltimo, T., Sener, B., & Stark, W. J. (2008). Do bioactive glasses convey a disinfecting mechanism beyond a mere increase in pH? *International Endodontic Journal, 41*(8), 670–678. https://doi.org/10.1111/j.1365-2591.2008.01413.x

[28] Wanitwisutchai, T., et al. (2021). Buffering capacity and antibacterial properties among bioactive glass-containing orthodontic adhesives. *Dental Materials Journal, 40*(5), 1169–1176. https://doi.org/10.4012/dmj.2020-375

[29] Li, A., et al. (2017). In vitro evaluation of a novel pH neutral calcium phosphosilicate bioactive glass that does not require preconditioning prior to use. *International Journal of Applied Glass Science, 8*(4), 403–411. https://doi.org/10.1111/ijag.12321

[30] Silver, I. A., & Erecinska, M. (2003). Interactions of osteoblastic and other cells with bioactive glasses and silica in vitro and in vivo. *Materialwissenschaft und Werkstofftechnik, 34*(12), 1069–1075. https://doi.org/10.1002/mawe.200300710

[31] Yusof, N. N., Aziz, S. M., Noor, F. M., Yaacob, S. N. S., & Hashim, S. (2022). A novel borate-based 45S5 Bioglass®: In vitro assessment in phosphate-buffered saline solution. *Journal of Non-Crystalline Solids, 596*, 121843. https://doi.org/10.1016/j.jnoncrysol.2022.121843

[32] Zehnder, M., Baumgartner, G., Marquardt, K., & Paqué, F. (2007). Prevention of bacterial leakage through instrumented root canals by bioactive glass S53P4 and calcium hydroxide suspensions in vitro. *Oral Surgery, Oral Medicine, Oral Pathology, Oral Radiology, and Endodontology, 103*(3), 423–428. https://doi.org/10.1016/j.tripleo.2006.10.021

[33] Kayıran, H. F. (2026). Thermo-Elastic Analysis of an Axisymmetric Layered Cylinder under Constant Thermal Loading with Artificial Intelligence-Based Validation. *Intelligent Systems Research and Applications Journal*, *2*, 76-89. https://doi.org/10.59543/0x8ky937

[34] Yaseen Mushtaq, Wajid Ali, Usman Ghani, Rahim Ullah Khan, & Amal Kumar Adak. (2025). Advancing Aviation Safety and Sustainable Infrastructure: High-Accuracy Detection and Classification of Foreign Object Debris Using Deep Learning Models. *International Journal of Sustainable Development Goals*, *1*, 82-98. https://doi.org/10.59543/ijsdg.v1i.14279

[35] Rahim Ullah, Muhammad Saeed, Wajid Ali, Junaid Nazar, & Fakhra Nazar. (2025). A Cooperative Heterogeneous Multi-Agent System Leveraging Deep Reinforcement Learning. *Knowledge and Decision Systems With Applications*, *1*, 112-124. https://doi.org/10.59543/kadsa.v1i.13931